Hole properties of the mixed-dimensional t-$J_\perp$-ladder from series expansions

Bachelorarbeit aus der Physik

Vorgelegt von
Jakob Heidweiler
9. Februar 2024

Lehrstuhl für Theoretische Physik V
Friedrich-Alexander-Universität Erlangen-Nürnberg

Betreuer: Prof. Dr. Kai Phillip Schmidt

Abstract

In this Bachelor's thesis, we study a mixed-dimensional t-$J_\perp$-ladder doped with one hole, with a hole-hopping parameter t along the legs and magnetic coupling $J_\perp$ in the dimers forming the rungs. Using perturbative continuous unitary transformations (pCUTs) around the limit of isolated rungs, we transform the Hamiltonian into an effective one, separating the magnetic and hole sector. We then diagonalize it by applying a Fourier transformation and study the gap between the ground-state energy and the minimal energy of the one-hole dispersion up to order 15 in the perturbation paramter $\lambda = t/J_\perp$. Next, we extrapolate the series using Padé and Dlog Padé approximations, which allows us to locate the quantum critical point $\lambda_c = 0.5285693 \pm 0.0000007$ in a quantitative fashion. Finally, we determine the power law according to which the gap closes to be $z\nu = 1.000 \pm 0.001$.

Contents

1. Introduction

Ever since the discovery of superconductivity in 1911 by Onnes [1], researchers have set out to find a superconductor that works at room temperature and atmospheric pressure. A major milestone in this quest was the discovery of the first high-temperature (high-T) superconductor in 1983 [2]. While BCS theory (1957), based on electron-phonon interactions, successfully explains the formation of Cooper pairs in conventional superconductors [3, 4], the precise pairing mechanism in high-T superconductors remains unknown, despite extensive research over the last few decades. One of the models suggested as the basis upon which to discuss these high-T superconducting systems is the t-J-model [5], i.e., magnetic interactions in doped Mott isolators are expected to be key.

So called mixed-dimensional t-J-models, where magnetic pairing and charge movement take place in separate dimensions have recently been suggested as a foundation for exploring properties of doped Mott isolators [6]. Ref. [7] even suggests that the high-T nickelate superconductor $La_3Ni_2O_7$ can be modelled by a system of mixed-dimensional bilayers. Because of the mixed dimensionality, these systems are considerably easier to handle both numerically and analytically.

Ladder systems are an additional simplification of a lattice layer down to quasi one dimension. Despite their apparent simplicity, they are used to model the structure of existing materials, especially cuprate compounds [8], where they are combined into a more complex structure. In the setting of a t-J-ladder, magnetic pairing mechanisms have already been found [9, 10]. Recent works on mixed-dimensional t-$J_\perp$-ladder systems also suggest a magnetic pairing mechanism between holes on opposite legs of the ladder [11, 12], after studying it using density matrix renormalization group (DMRG) calculations. An experimental realization of mixed-dimensional t-$J_\perp$-ladders has been achieved recently, using a quantum gas of ultracold atoms, which confirmed a magnetic pairing mechanism [13].

The experimental finding of a magnetically mediated pairing mechanism between holes is an important development, because it strengthens the validity of the microscopic modeling. To better understand the behaviour of holes in such a system as in Ref. [12], we extend the investigation of mixed-dimensional t-$J_\perp$-ladders by first studying isolated rungs and then deriving the full model perturbatively from the limit of small coupling between the rungs. In the past, this method has already been applied successfully to ladder systems [14]. We limit our study to a system with only one hole and therefore omit the hole-hole repulsion present in Ref. [12].

We begin by introducing the model from the limit of isolated dimers and from that construct a mixed-dimensional t-$J_\perp$-ladder. We calculate the hopping processes of one hole in chapter 2 and rewrite the Hamiltonian in a form that allows us to study the system using perturbative continuous unitary transformations (pCUTs). Next, we explain the

fundamentals of pCUTs and take a look at extrapolation methods aimed at extracting quantum-critical properties in chapter 3. Then, we present our results on the one hole dispersion and quantum phase transition in chapter 4 and conclude the thesis in chapter 5 by summarizing the results and giving an outlook on remaining questions.

2. Model

In this chapter we introduce the model of a mixed-dimensional t-$J_\perp$-ladder. First, we explain the properties of a single isolated dimer in section 2.1. Then, from the limit of multiple isolated dimers, we study the mixed-dimensional t-$J_\perp$-ladder in detail in section 2.2.

2.1. Isolated Dimer

An isolated dimer consists of two sites, which are either empty or carry a spin-$\frac{1}{2}$. The spins interact magnetically via a Heisenberg coupling and are thus described by the Hamiltonian

$$H = J_\perp \vec{S}_1 \cdot \vec{S}_2 \,, \tag{2.1}$$

with the antiferromagnetic coupling strength $J_\perp > 0$ and the spin operator $\vec{S}_i$ at position i. We can expand this into

$$H = J_\perp \left(S_1^x S_2^x + S_1^y S_2^y + S_1^z S_2^z \right) \tag{2.2}$$

and then simplify it further using the ladder operators $S_i^\pm = S_i^x \pm \mathrm{i} S_i^y$. The result is

$$H = J_\perp \left(\frac{1}{2} \left(S_1^+ S_2^- + S_1^- S_2^+ \right) + S_1^z S_2^z \right) . \tag{2.3}$$

Because this Hamiltonian is not diagonal in the subspace of only spins and no holes with product basis $\{|\uparrow\uparrow\rangle, |\uparrow\downarrow\rangle, |\downarrow\uparrow\rangle, |\downarrow\downarrow\rangle\}$, we need to diagonalize it. The resulting eigenstates and corresponding energies are

$$|s\rangle \coloneqq \frac{1}{\sqrt{2}} \left(|\uparrow\downarrow\rangle - |\downarrow\uparrow\rangle \right) \qquad E_{|s\rangle} = -\frac{3}{4} J_\perp \tag{2.4}$$

$$\left|t^{+1}\right\rangle \coloneqq |\uparrow\uparrow\rangle \qquad E_{|t^{+1}\rangle} = \frac{1}{4} J_\perp \tag{2.5}$$

$$\left|t^{0}\right\rangle \coloneqq \frac{1}{\sqrt{2}} \left(|\uparrow\downarrow\rangle + |\downarrow\uparrow\rangle \right) \qquad E_{|t^{0}\rangle} = \frac{1}{4} J_\perp \tag{2.6}$$

$$\left|t^{-1}\right\rangle \coloneqq |\downarrow\downarrow\rangle \qquad E_{|t^{-1}\rangle} = \frac{1}{4} J_\perp \,. \tag{2.7}$$

We notice that the singlet state $|s\rangle$, carrying total spin $s = 0$, is the ground state. The triplet states $|t^\alpha\rangle$ all carry total spin $s = 1$ and are differentiated by their quantum number $\alpha \in \{+1, 0, -1\}$. Because they all have the same energy, they are three-fold degenerate eigenstates.

If we remove one of the spins in the dimer, a so called hole is created, which we denote by o. For both one and two holes in the dimer, no interaction takes place and thus the energy of the dimer becomes 0. The states with holes are therefore already eigenstates of the Hamiltonian in Equation 2.3. The energy spectrum of a dimer for all nine possible states can be seen in Figure 2.1a for $J_\perp = 1$.

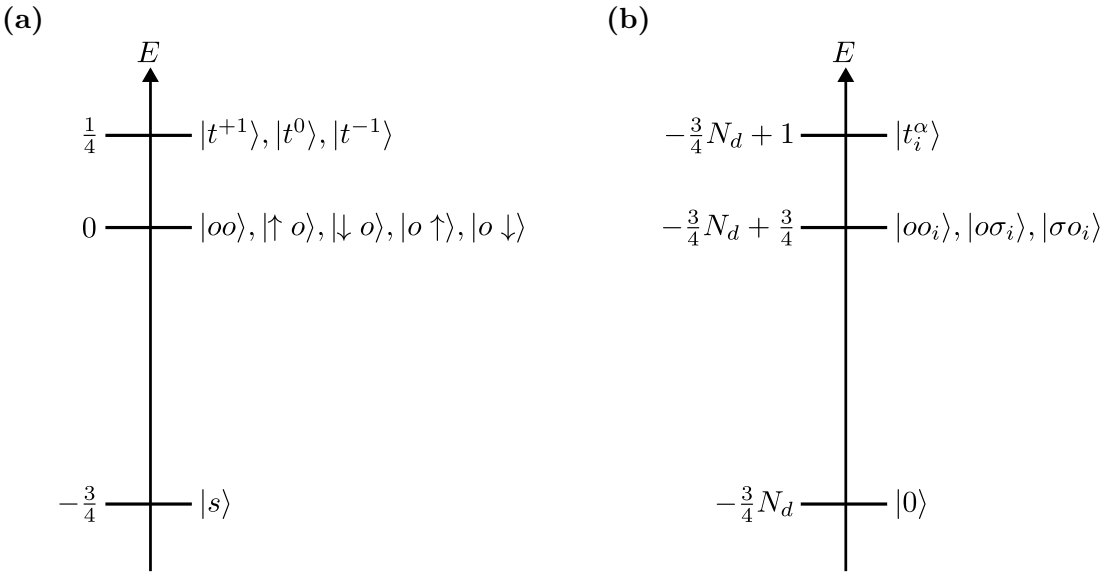

Figure 2.1.: Energy spectra of one dimer (a) and N_d isolated dimers (b) for intra-dimer coupling $J_\perp = 1$. For one dimer, the ground state is the singlet $|s\rangle$. The triplet states are $|t^\alpha\rangle$, with $\alpha \in \{+1, 0, -1\}$ and holes in a dimer are denoted as o. For multiple dimers, the ground state of all singlets is given by $|0\rangle$. The first excitation is reached, when one of the singlets is doped with one or two holes o. The second excitation corresponds to a local triplet $|t^\alpha\rangle$ and no holes.

For a system consisting of N_d uncoupled dimers, the eigenstates are separable and we can write them as product states of the individual dimer states

$$\bigotimes_{i=1}^{N_d} |...\rangle_i = |...\rangle_1 \otimes ... \otimes |...\rangle_{N_d} . \tag{2.8}$$

We can then calculate its energy by summing up the energies of the individual dimers. Since the energy of a dimer with one and two holes is degenerate, adding a second hole to a dimer does not change the energy of the system. Therefore, the energy of N_d dimers, where N_t is the number of triplet states and N_o is the number of dimers with at least one hole, is given by

$$\begin{aligned} E &= \sum_{n=1}^{N_d - N_t - N_o} \left(-\frac{3}{4} J_\perp \right) + \sum_{n=1}^{N_t} \frac{1}{4} J_\perp + \sum_{n=1}^{N_o} 0 \cdot J_\perp \\ &= -\frac{3}{4} J_\perp N_d + J_\perp N_t + \frac{3}{4} J_\perp N_o . \end{aligned} \tag{2.9}$$

The system's ground state is

$$\bigotimes_{i=1}^{N_d} |s\rangle_i \,, \tag{2.10}$$

because the energy is minimized, when every dimer is in its singlet state $|s\rangle$. According to Equation 2.9 we get the ground-state energy

$$E_0 = \sum_{i=1}^{N_d} \left(-\frac{3}{4} J_\perp \right) = -\frac{3}{4} J_\perp N_d \,. \tag{2.11}$$

We can reach the first excitation by doping one singlet with one or two holes o, because this increases the energy by only $\frac{3}{4}J_\perp$, where instead exciting a singlet to a triplet increases the energy by $J_\perp$. In this thesis, we are interested in the low-energy properties of a mixed-dimensional t-$J_\perp$-ladder and are therefore working with states, that are close to the ground state and only contain a few excitations. Thus, it is reasonable to denote a state by only giving the excitations and to ignore the underlying singlet background. A state is then given by the ket

$$\left| o\sigma_i, t^\alpha_{i+1}, ... \right\rangle , \tag{2.12}$$

where only the dimers with holes o and spin $\sigma \in \{\uparrow, \downarrow\} = \{+\frac{1}{2}, -\frac{1}{2}\}$ and the the triplets $|t^\alpha\rangle$ are given, ordered by their index i. Using this notation, the energy spectrum is displayed in Figure 2.1b.

2.2. Mixed-dimensional t-$J_\perp$-Ladder

From the limit of N_d isolated dimers from section 2.1, we can now construct the mixed-dimensional t-$J_\perp$-ladder by coupling them with a hopping parameter t. As displayed in Figure 2.2, the system now consists of dimers with magnetic Heisenberg coupling $J_\perp$ in effectively zero dimensions. They are located at positions $i = 1, ..., N_d$ and form

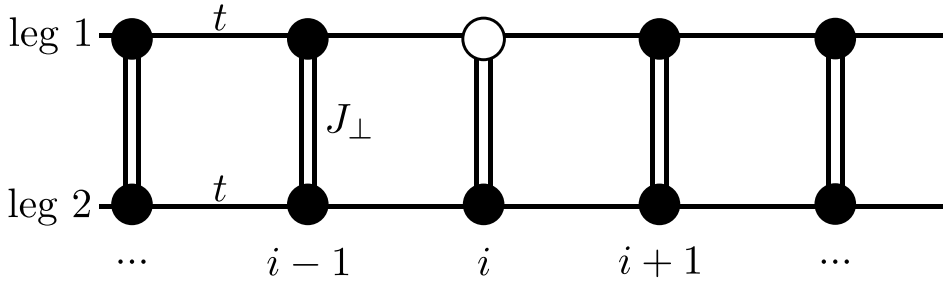

Figure 2.2.: A mixed-dimensional t-$J_\perp$-ladder. The rungs are N_d dimers consisting of spins (filled circles) and holes (empty circles). The intra-dimer coupling is denoted $J_\perp$. The legs of the ladder are formed by the hopping parameter t between dimers, that allows for nearest-neighbour hopping of the holes along the legs. The position of a rung is denoted by the index $i = 1, ..., N_d$.

the rungs of the two-leg ladder. They consist of either spins (filled circles) or holes

(empty circles). The hopping parameter t allows for holes to hop along the legs to the position of its nearest-neighbour dimers, but not inside the dimer itself. Effectively, this forms a one-dimensional chain along which the holes can move. Hence the name mixed-dimensional t-$J_\perp$-ladder.

Obviously, for $t = 0$, the system of uncoupled dimers, described in section 2.1, is recovered. For $t \neq 0$, however, the Hamiltonian for this system is given by

$$\begin{aligned} H &= J_\perp H_\perp + tH_t \\ &= J_\perp \sum_i^{N_d} \vec{S}_{i,1}\vec{S}_{i,2} + t\sum_i^{N_d}\sum_{\sigma\in\{\uparrow,\downarrow\}} \left(b^\dagger_{i+1,1,\sigma} b_{i,1,\sigma} + b^\dagger_{i+1,2,\sigma} b_{i,2,\sigma} + \text{h.c.}\right) \end{aligned} \tag{2.13}$$

in second quantization. Here, $J_\perp$ is the coupling strength along the rungs, N_d is the total number of rungs, $\vec{S}_{i,\nu}$ is the spin operator for site (i,ν), $\nu \in \{1,2\}$ is the index for the legs of the ladder, and t is the hopping parameter. The operators $b^\dagger_{i,\nu,\sigma}$ and $b_{i,\nu,\sigma}$ are hard-core bosonic hole creation and annihilation operators. The creation operators behave according to

$$b^\dagger_{i,1,\sigma}|\tilde{\sigma}\rho\rangle = \delta_{\sigma,\tilde{\sigma}}|o\rho\rangle \qquad b^\dagger_{i,2,\sigma}|\rho\tilde{\sigma}\rangle = \delta_{\sigma,\tilde{\sigma}}|\rho o\rangle \tag{2.14}$$

$$b^\dagger_{i,1,\sigma}|o\rho\rangle = 0 \qquad b^\dagger_{i,2,\sigma}|\rho o\rangle = 0 \tag{2.15}$$

and the annihilation operators as

$$b_{i,1,\sigma}|o\rho\rangle = |\sigma\rho\rangle \qquad b_{i,2,\sigma}|\rho o\rangle = |\rho\sigma\rangle \tag{2.16}$$

$$b_{i,1,\sigma}|\rho o\rangle = 0 \qquad b_{i,2,\sigma}|o\rho\rangle = 0\,, \tag{2.17}$$

with the spins $\sigma, \tilde{\sigma}, \rho \in \{\uparrow,\downarrow\}$. That means, the operator $b^{(\dagger)}_{i,\nu,\sigma}$ will annihilate (create) a hole in the ith dimer and in the νth leg of the ladder and create (annihilate) a spin σ in the process. They follow the hard-core bosonic commutator relations [15]

$$\begin{aligned} \left[b_{i,\nu,\sigma}, b^\dagger_{j,\mu,\sigma}\right] &= \delta_{i,j}\delta_{\mu,\nu}\left(\mathbb{1} - 2n_{i,\nu,\sigma}\right) \\ \left[b_{i,\nu,\sigma}, b_{j,\mu,\sigma}\right] &= 0 \\ \left[b^\dagger_{i,\nu,\sigma}, b^\dagger_{j,\mu,\sigma}\right] &= 0\,, \end{aligned} \tag{2.18}$$

with the commutator $[A,B] = AB - BA$ and the counting operator $n_{i,\nu,\sigma} = b^\dagger_{i,\nu,\sigma} b_{i,\nu,\sigma}$.

The Hamiltonian in Equation 2.13 can be written as the sum of two independent Hamiltonians: $H_\perp$ for the intra-dimer coupling and H_t for the coupling between dimers, i.e., the hopping of holes. The magnetic part $H_\perp$ is already diagonal in our dimer basis and its energy is given by Equation 2.9. The part of particular interest is H_t, the hopping Hamiltonian. We notice that the ground state for uncoupled dimers in Equation 2.10 is not affected by H_t, as it contains no holes. Therefore, it is an exact eigenstate of the Hamiltonian H in Equation 2.13. For small t, it is also the ground state, however, only up to a certain ratio of $t/J_\perp =: \lambda_c$, where the energy of the one-hole system becomes

smaller. Therefore, adding just one hole already leads to interesting effects, which we will study in chapter 4.

Because we only have nearest-neighbour hopping, we start by looking at a system with a total number of dimers $N_d = 2$ and exactly one hole. From Equation 2.13 we then get the hopping Hamiltonian

$$H_t = \sum_{i=1}^{2} \sum_{\sigma\in\{\uparrow,\downarrow\}} \left(b^\dagger_{i+1,1,\sigma} b_{i,1,\sigma} + b^\dagger_{i+1,2,\sigma} b_{i,2,\sigma} + \text{h.c.} \right) . \tag{2.19}$$

We can see, that it can be separated into terms describing the hopping in leg 1 and in terms describing hopping in leg 2. Therefore, it is justified to only look at the hopping process in leg 1. Our system now has a total number of 16 different relevant states, described by

$$|o\sigma\rangle \otimes |s\rangle \qquad |o\sigma\rangle \otimes |t^\alpha\rangle \qquad |s\rangle \otimes |o\sigma\rangle \qquad |t^\alpha\rangle \otimes |o\sigma\rangle \,, \tag{2.20}$$

with $\sigma \in \{+\frac{1}{2}, -\frac{1}{2}\}$ and $\alpha \in \{+1, 0, -1\}$.

By applying H_t to every state, we find the following processes for hopping to the right

$$\begin{aligned}
|o\sigma\rangle \otimes |s\rangle &\xrightarrow{H_t} 2\sigma\frac{1}{\sqrt{2}}\left|t^{2\sigma}\right\rangle \otimes |o{-}\sigma\rangle - 2\sigma\frac{1}{2}\left|t^{0}\right\rangle \otimes |o\sigma\rangle + \frac{1}{2}|s\rangle \otimes |o\sigma\rangle \\
|o\sigma\rangle \otimes \left|t^{2\sigma}\right\rangle &\xrightarrow{H_t} \left|t^{2\sigma}\right\rangle \otimes |o\sigma\rangle \\
|o\sigma\rangle \otimes \left|t^{-2\sigma}\right\rangle &\xrightarrow{H_t} -2\sigma\frac{1}{\sqrt{2}}|s\rangle \otimes |o{-}\sigma\rangle + \frac{1}{\sqrt{2}}\left|t^{0}\right\rangle \otimes |o{-}\sigma\rangle \\
|o\sigma\rangle \otimes \left|t^{0}\right\rangle &\xrightarrow{H_t} -\sigma\frac{1}{2}|s\rangle \otimes |o\sigma\rangle + \frac{1}{2}\left|t^{0}\right\rangle \otimes |o\sigma\rangle + \frac{1}{\sqrt{2}}\left|t^{2\sigma}\right\rangle \otimes |o{-}\sigma\rangle \,.
\end{aligned} \tag{2.21}$$

Since Equation 2.19 can be further separated into terms describing hopping to the left and hopping to the right, hopping to the left is described by simply exchanging the factors of the tensor product $\otimes$.

We notice, that H_t conserves the hole number and the total magnetization of our system. More interestingly, H_t is not diagonal in our states in Equation 2.20, because they hybridize with other states under H_t. That is because although H_t contains only terms describing the hopping of the holes, it can also create/annihilate magnetic excitations $|t^\alpha\rangle$. As a result, we can no longer calculate the energy using Equation 2.9. Therefore, we use a perturbative approach around the limit of isolated dimers. The expansion around this case only allows us to study situations where the hole-hopping is much smaller than the magnetic coupling, i.e., $t \ll J_\perp$.

Let us therefore rewrite the Hamiltonian from Equation 2.13 into the dimensionless form of

$$H = H_0 + \lambda V \,. \tag{2.22}$$

Here, H_0 is the magnetic Hamiltonian $H_\perp$. The perturbation V is the hopping Hamiltonian H_t and the perturbation parameter is given by $\lambda = t/J_\perp$. Because $t \ll J_\perp$, it follows that $\lambda \ll 1$. There are many different frameworks in which to do perturbative

calculations [16, 17, 18]. In this thesis we use perturbative continuous unitary transformations (pCUTs) [19], since we can use a numerical "Solver" programme [20] to automate high-order calculations. For this, we rewrite V, using operators T_n which create n triplet excitations $|t^\alpha\rangle$ and fulfil $[H_0, T_n] = nT_n$, into

$$V = T_{-1} + T_0 + T_{+1}\,. \tag{2.23}$$

The operators T_n take the form

$$T_n = \sum_i \tau_n^i\,, \tag{2.24}$$

with the local operators τ_n^i, which create n quasiparticles acting on the bond between rung i and $i+1$. The actions of the operators τ_n^i are given in Table 2.1. In section 3.1 of

	τ_0^i	
$\|o\sigma\rangle_i \otimes \|s\rangle_{i+1}$	$\longrightarrow$	$\frac{1}{2}\|s\rangle_i \otimes \|o\sigma\rangle_{i+1}$
$\|o\sigma\rangle_i \otimes \|t^{2\sigma}\rangle_{i+1}$	$\longrightarrow$	$\|t^{2\sigma}\rangle_i \otimes \|o\sigma\rangle_{i+1}$
$\|o\sigma\rangle_i \otimes \|t^{-2\sigma}\rangle_{i+1}$	$\longrightarrow$	$\frac{1}{\sqrt{2}}\|t^0\rangle_i \otimes \|o{-}\sigma\rangle_{i+1}$
$\|o\sigma\rangle_i \otimes \|t^0\rangle_{i+1}$	$\longrightarrow$	$\frac{1}{\sqrt{2}}\|t^{2\sigma}\rangle_i \otimes \|o{-}\sigma\rangle_{i+1} + \frac{1}{2}\|t^0\rangle_i \otimes \|o\sigma\rangle_{i+1}$
	τ_{+1}^i	
$\|o\sigma\rangle_i \otimes \|s\rangle_{i+1}$	$\longrightarrow$	$2\sigma\frac{1}{\sqrt{2}}\|t^{2\sigma}\rangle_i \otimes \|o{-}\sigma\rangle_{i+1} - 2\sigma\frac{1}{2}\|t^0\rangle_i \otimes \|o\sigma\rangle_{i+1}$

Table 2.1.: Actions of the local operators τ_n^i from Equation 2.24.

the next chapter, we explain the details of pCUTs.

3. Method

We apply different methods to study the behaviour of one hole in a mixed-dimensional t-$J_\perp$-ladder, which we will explain in this chapter. First, we explain the details of perturbative continuous unitary transformations (pCUTs) in section 3.1, which we use to transform our Hamiltonian from Equation 2.13 into an effective blockdiagonal Hamiltonian H_{eff}. Then we detail Padé and Dlog Padé approximations in section 3.2, which allow us to extrapolate the power series of the energy gap $\Delta(\lambda)$ of a single hole.

3.1. Perturbative Continuous Unitary Transformations (pCUTs)

The basic idea of pCUTs is to transform a given non diagonal Hamiltonian into a block diagonal effective Hamiltonian H_{eff}. For this, continuous unitary transformations (CUTs) are used to formulate a flow equation for H which is then solved perturbatively. This can be done, if our system is described by a Hamiltonian H, that can be written as

$$H = H_0 + \lambda V\,, \tag{3.1}$$

where H_0 is the unperturbed Hamiltonian, V is the perturbation, λ with $\lambda < 1$ is the perturbation parameter, and the following two conditions are fulfilled:

1. H_0 has an equidistant energy spectrum and is bounded from below.
2. V can be written as
$$V = \sum_{n=-N}^{N} T_n \tag{3.2}$$
where T_n increments the number of energy quanta by n and fulfils $[H_0, T_n] = nT_n\,.$

We can get an expression for H_{eff} by using the CUT

$$H(l) = U^\dagger(l) H U(l)\,, \tag{3.3}$$

with a flow parameter $l \in \mathbb{R}$ such that

$$H(0) = H \tag{3.4}$$
$$\lim_{l\to\infty} H(l) = H_{\text{eff}}\,. \tag{3.5}$$

We can find H_{eff} by solving the flow equation

$$\frac{dH(l)}{dl} = [\eta(l), H(l)]\,, \tag{3.6}$$

with an antihermitian infinitesimal generator $\eta(l)$, that engenders the unitary evolution [19]. For it, we use the quasi-particle-generator

$$\eta_{\text{qp}}(l) = \text{sgn}(q_i(l) - q_j(l))H_{ij}(l)\,, \tag{3.7}$$

with the q_i being the eigenvalues of the particle counting operator Q in its eigenbasis $\{|i\rangle\}$. Equation 3.6, together with the perturbative ansatz from Equation 3.1 and the generator from Equation 3.7, gives a system of coupled differential equations, that can be solved in a perturbative manner. Details on the solution can be found in [19]. The resulting effective Hamiltonian is then given by

$$H_{\text{eff}} = H_0 + \sum_{k=1}^{\infty} \lambda^k \sum_{|\vec{m}|=k,\, M(\vec{m})=0} C(\vec{m})T(\vec{m})\,, \tag{3.8}$$

with

$$\vec{m} = (m_1, m_2, ...m_k) \quad \text{with} \tag{3.9}$$
$$m_i \in \{-N, ..., 0, ..., N\} \tag{3.10}$$
$$|\vec{m}| = k \tag{3.11}$$
$$T(\vec{m}) = T_{m_1} T_{m_2} ... T_{m_k} \tag{3.12}$$
$$M(\vec{m}) = \sum_{i=1}^{k} m_i\,. \tag{3.13}$$

Once calculated, the coefficients $C(\vec{m})$ are independent of the model and the solution for H_{eff} therefore is valid for all systems fulfilling the conditions above. Since they are model independent, the coefficients were already available at the onset of this thesis, as well as a "Solver" programme [20]. Therefore, to apply the pCUT method to the mixed-dimensional t-$J_\perp$-ladder, we need to find the specific form and actions of the operators T_n, that take the form

$$T_n = \sum_i \tau_n^i\,, \tag{3.14}$$

with the operators τ_n^i which create n quasiparticles acting on the bond between dimer i and $i+1$.

We have found the T_n already in chapter 2 and have, in principle, already obtained the block-diagonal effective Hamiltonian. However, it is hard to determine the physical meaning of the T_n operator sequences. That is the reason, why we rewrite the effective Hamiltonian into a normal-ordered H_{eff} in chapter 4, using different operators.

3.2. Extrapolation

In chapter 4, we calculate a power series of the gap $\Delta(\lambda)$. To find the point where a quantum phase transition occurs, we want to locate the critical point λ_c where the gap closes, i.e., where $\Delta(\lambda_c) = 0$. Furthermore, assuming a second-order phase transition, we know that Δ closes according to some power law and is proportional to

$$\Delta(\lambda) \propto |\lambda - \lambda_c|^{z\nu} = \left(\frac{\lambda}{\lambda_c} - 1\right)^{z\nu} \tag{3.15}$$

for $\lambda > \lambda_c$. The critical exponent $z\nu$ is of interest to us, because we can use it to validate whether we can use Padé approximants to determine λ_c. It is further relevant to narrow down the possibilities for the universality class of the quantum phase transition [21]. However, the series we calculated for $\Delta(\lambda)$ only converges up to a certain point, making it impossible to find λ_c and $z\nu$. Nonetheless, we can extend the series by extrapolating it using Padé and Dlog Padé approximations, allowing for assessment of the behaviour at the critical point. Below, first the details of Padé approximation are introduced, followed by an explanation of Dlog Padé approximation.

Padé extrapolation

The Taylor series of a function $f(x) \approx \mathcal{T}_f(x) = \sum_{n=0}^{r} b_n x^n$ of order r can be approximated by the ratio of two polynomials $P_L(x)$ and $Q_M(x)$

$$\sum_{n=0}^{r} b_n x^n = \frac{P_L(x)}{Q_M(x)} = \frac{p_0 + p_1 x + ... + p_L x^L}{1 + q_1 x + ... + q_M x^M} =: \mathrm{P}[L, M]_{\mathcal{T}_f} \tag{3.16}$$

called a Padé approximant [22]. The degrees L and M of P_L and Q_M must satisfy the relation $L + M \leq r$. We can determine the coefficients p_i and q_i by equating coefficients of equal power of x in the equation

$$P_L(x) = \mathcal{T}_f(x) Q_M(x) \tag{3.17}$$

and solving the resulting system of linear equations [23]. The resulting approximation of $f(x)$ converges better than its Taylor series.

In order to determine the quality of our extrapolation of Δ, we calculate multiple Padé approximants and their roots x_c for different values of L and M and examine if they behave similarly. Some of the approximants have poles of non-physical origin in a complex interval I around an educated guess for the critical point λ_c, leading to additional roots. Because they effect the accuracy of the physical root, we exclude them and call them defective. Because the quality of the approximants generally decreases with a larger difference between L and M, we use only those with $|L - M| \leq 3$ and arrange them in so called families of $L - M = \text{const}$. Padé approximants can only describe integer power laws near the critical point λ_c [24]. This is not necessarily the case in our system. It is therefore also necessary to extrapolate $\Delta(\lambda)$ using Dlog Padé approximation which is able to describe non-integer critical exponents.

Dlog Padé extrapolation

The Dlog Padé approximant of the Taylor series $\mathcal{T}_f(x)$ from Equation 3.16 can be defined by first approximating the derivative of the natural logarithm of $\mathcal{T}_f(x)$

$$\frac{d}{dx}\ln(\mathcal{T}_f(x)) = \frac{\frac{d}{dx}\mathcal{T}_f(x)}{\mathcal{T}_f(x)} = \frac{P_L(x)}{Q_M(x)} =: \mathrm{P}[L,M]_{\frac{d\ln(\mathcal{T}_f)}{dx}}\,. \tag{3.18}$$

The resulting differential equation

$$\frac{d}{dx}\mathcal{T}_f(x) = \frac{P_L(x)}{Q_M(x)}\mathcal{T}_f(x) \tag{3.19}$$

can be solved for $\mathcal{T}_f$

$$\mathcal{T}_f(x) = e^{\int_0^x \frac{P_L(x')}{Q_M(x')}\mathrm{d}x'} =: \mathrm{dP}[L,M]\,, \tag{3.20}$$

which results in the Dlog Padé approximant $\mathrm{dP}[L,M]$. The roots x_c of $\mathrm{dP}[L,M]$ are then given by the roots of $Q_M(x')$.

If $f(x)$ follows a power law as in Equation 3.15, then the critical exponent $z\nu$ is given by the residuum of $\frac{P_L(x)}{Q_M(x)}$

$$z\nu = \left.\frac{P_L(x)}{\frac{d}{dx}Q_M(x)}\right|_{x=x_c}\,. \tag{3.21}$$

To determine λ_c, we again extrapolate Δ for different values of L and M with $|L-M| \leq 3$ using Dlog Padé approximation and filter out defective ones as described above. We calculate λ_c from the remaining Dlog Padé approximants and examine whether each family converges to the same value. Finally, we then average over the value of highest order in each family to determine the definitive λ_c with an uncertainty that is given by the standard deviation of the average. The critical exponent according to Equation 3.21 is then determined likewise.

4. Results: One-Hole Sector

Our goal for this thesis is to understand the behaviour of holes in a mixed-dimensional t-$J_\perp$-ladder from section 2.2. Here, we study the system with exactly one hole. We use pCUTs to transform our Hamiltonian into a block-diagonal effective Hamiltonian H_{eff}, that conserves the number of triplet excitations and therefore allows us to extract physical properties of the holes in the absence of triplet excitations. The one-hole sector then contains only hopping terms. In section 4.1, we manually derive, in the first two orders, a normal-ordered form of our effective Hamiltonian in the one-hole sector. Then we use a "Solver" programme in section 4.2 to calculate H_{eff} in the one-hole sector up to order 15. In section 4.3, we diagonalize the effective Hamiltonian using Fourier transformations and determine the dispersion relation $\omega(k)$ of the hole. In the last step, we calculate the energy gap $\Delta(\lambda)$ between the ground state for $t = 0$ and the energy for a mixed-dimensional t-$J_\perp$-ladder with one hole. We locate quantitatively the quantum phase transition point λ_c and determine the associated critical exponent $z\nu$ in section 4.4.

4.1. Leading-Order Perturbative Calculations

To understand the behaviour of one hole in a mixed-dimensional t-$J_\perp$-ladder we recall the Hamiltonian from Equation 2.13, its dimensionless form Equation 2.22 and the operators in Table 2.1. The leading two orders of the effective Hamiltonian H_{eff} are given by

$$H_{\text{eff}} = H_0 + \lambda T_0 + \lambda^2(-T_{-1}T_{+1} + T_{+1}T_{-1}) + \mathcal{O}(\lambda^3)\,. \tag{4.1}$$

We recall Equation 3.14, that says that the operators T_n are a sum of local operators τ_n^i acting on the bond between the dimers i and $i+1$. Using the notation from Equation 2.12, the state of one hole in leg 1 and spin σ in leg 2 of dimer i and no magnetic excitations anywhere in the system, is denoted as

$$|o\sigma_i\rangle\,. \tag{4.2}$$

Applying the terms in Equation 4.1 individually, we get

$$\begin{aligned}
T_0|o\sigma_i\rangle &= \frac{1}{2}\left(|o\sigma_{i+1}\rangle + |o\sigma_{i-1}\rangle\right) , \\
-T_{-1}T_{+1}|o\sigma_i\rangle &= -T_{-1}\left[2\sigma\frac{1}{\sqrt{2}}\left|t_i^{2\sigma}, o{-}\sigma_{i\pm1}\right\rangle - 2\sigma\frac{1}{2}\left|t_i^0, o\sigma_{i\pm1}\right\rangle\right] \\
&= -\left[2\sigma\frac{1}{\sqrt{2}}\cdot 2\cdot 2\sigma\frac{1}{\sqrt{2}}|o\sigma_i\rangle - 2\sigma\frac{1}{2}\cdot 2\cdot(-2\sigma)\frac{1}{2}|o\sigma_i\rangle\right] \\
&= -\left[|o\sigma_i\rangle + \frac{1}{2}|o\sigma_i\rangle\right] \\
&= -\frac{3}{2}|o\sigma_i\rangle , \\
T_{-1}T_{+1}|o\sigma_i\rangle &= 0 .
\end{aligned} \tag{4.3}$$

We can identify the following coefficients $\tilde{a}_n$

$$\begin{aligned}
\tilde{a}_0 &= \langle o\sigma_i|V|o\sigma_i\rangle = -\frac{3}{2}\lambda^2 \\
\tilde{a}_{+1} &= \langle o\sigma_{i+1}|V|o\sigma_i\rangle = \frac{1}{2}\lambda \\
\tilde{a}_{-1} &= \langle o\sigma_{i-1}|V|o\sigma_i\rangle = \frac{1}{2}\lambda ,
\end{aligned} \tag{4.4}$$

that describe the transition amplitudes $\tilde{a}_n$ of the hole hopping by n places. We notice that $\tilde{a}_{+1} = \tilde{a}_{-1}$, because H is an hermitian operator and we therefore have the same processes for hopping to the right and hopping to the left. Therefore, we define $a_n \coloneqq \tilde{a}_{+n} = \tilde{a}_{-n}$ for $n > 0$. Additionally, we have to take into account that the full local hopping amplitude is given by

$$\begin{aligned}
\langle o\sigma_i|H_{\text{eff}}|o\sigma_i\rangle &= -\frac{3}{4}N_d + \frac{3}{4} - \frac{3}{2}\lambda^2 \\
&= E_0 + a_0
\end{aligned} \tag{4.5}$$

using the exact ground-state energy E_0 from Equation 2.11 and $a_0 \coloneqq \frac{3}{4} + \tilde{a}_0$. We use these coefficients to formulate the normal-ordered effective single-hole Hamiltonian

$$H_{\text{eff}} = E_0 + \sum_{i=1}^{N_d}\sum_{\nu=1}^{2}\sum_{\sigma\in\{\uparrow,\downarrow\}}\left[a_0 h_{i,\nu,\sigma}^\dagger h_{i,\nu,\sigma} + a_1\left(h_{i+1,\nu,\sigma}^\dagger h_{i,\nu,\sigma} + \text{h.c.}\right)\right] . \tag{4.6}$$

Because the operators $b_{i,\nu,\sigma}$ and $b_{i,\nu,\sigma}^\dagger$ from Equation 2.13 can lead to magnetic (de)excitations, we use different operators $h_{i,\nu,\sigma}^\dagger$ and $h_{i,\nu,\sigma}$. They are also hard-core bosonic operators, but create (annihilate) a hole o and spin $\sigma \in \{\uparrow,\downarrow\} = \{+\frac{1}{2}, -\frac{1}{2}\}$ together. They act on the ith dimer in the ladder that has a hole in leg ν and spin σ in the other leg. With this we have transformed our initial Hamiltonian, that coupled the hole sector and the magnetic sector into an effective Hamiltonian, that only contains terms describing the hopping of holes together with their spins. It is, however, still not fully diagonal, due to the nearest-neighbour hopping. Before we look at how we can diagonalize it, we first look at its form in higher orders.

4.2. Higher-Order Calculations

In the previous section, we saw that to determine a normal-ordered H_{eff} up to order r, we evaluated the effect of the T_n operator sequences from Equation 4.1 on the state with one hole and no triplets $|o\sigma_i\rangle$. In principle, we could use this to evaluate the higher orders by hand. This, however, becomes extremely tedious because the length and number of T_n sequences increases drastically with every order. Therefore, we use a "Solver" programme [20]. We need to specify the action of the τ_n^i operators and the programme will evaluate the a_n hopping contributions for us. Besides the action of the operators, the Solver still needs two things. First, it needs the coefficients $C(\vec{m})$ from Equation 3.8, which were available at the onset of this thesis[1]. Second, it needs the cluster, i.e., the exact spatial extension of the ladder, on which to evaluate the matrix elements of the effective Hamiltonian. We provide both by writing in configuration files. Designing the cluster is appropriately important. Choosing it too large can lead to longer computation times and large memory usage, because the programme has to store unnecessary sites. Even worse, choosing a cluster with too few sites can lead to wrong results, because of boundary effects as the hole reaches the ends of the cluster. We determine the shape of the cluster according to the following rules:

- For calculations in order r, we choose a cluster of size $r + 1$.
- For local hopping (coefficient a_0), we place the hole in site $i = \left\lceil \frac{r}{2} \right\rceil$ and evaluate it staying there.
- For hopping by n sites (a_n), we place the initial hole in the site $i = \left\lceil \frac{r}{2} \right\rceil + \left\lfloor \frac{n}{2} \right\rfloor$, and evaluate it reaching the site $j = \left\lceil \frac{r}{2} \right\rceil - \left\lceil \frac{n}{2} \right\rceil$.

Because we have nearest-neighbour hopping and thus the hole can move a maximum of r sites in order r, these rules ensure that we have the smallest cluster possible while still having as many sites as necessary to get correct results. Using this, we calculate the hopping amplitudes a_n, $n = 1, ..., 15$ in order $r = 15$. The full list can be found in Appendix A. We make the following observations. While $r = 1$, we only have terms describing the hopping of the hole by one site. Going to order 2 also gives us only a correction for local hopping (see section 4.1). From order 3 to 15, every new order r contributes to a_n with $n = r - 2k$, where $n \geq 0$, $k \in \mathbb{N}_{\neq 0}$, which is the reason why $a_{14} = a_{15} = 0$. With this we get the effective Hamiltonian

$$H_{\text{eff}} = E_0 + \sum_{i=1}^{N_d} \sum_{\nu=1}^{2} \sum_{\sigma \in \{\uparrow,\downarrow\}} \left[a_0 h^\dagger_{i,\nu,\sigma} h_{i,\nu,\sigma} + \sum_{n=1}^{r-2} a_n \left(h^\dagger_{i+n,\nu,\sigma} h_{i,\nu,\sigma} + \text{h.c.} \right) \right], \tag{4.7}$$

which in order $r = 2$ is identical to Equation 4.6. Again, we have transformed our initial Hamiltonian into a normal-ordered effective Hamiltonian in the single-hole sector, that only contains terms describing the hopping of the hole together with the spin in the same rung. This Hamiltonian, however, is not diagonal, as it has entries on the nth diagonals

[1]The coefficients $C(\vec{m})$ for order one to ten can be found in Ref. [19].

in the real-space basis, that stem from the hopping by n sites. In the next section we will diagonalize the Hamiltonian using Fourier transformation.

4.3. Dispersion

We diagonalize the effective Hamiltonian from Equation 4.7 by going into momentum space using the Fourier transform $\mathcal{F}$. The operators transform in the following way

$$h^\dagger_{j,\nu,\sigma} = \frac{1}{\sqrt{N_d}} \sum_k e^{-\mathrm{i}kj} h^\dagger_{k,\nu,\sigma} \qquad\qquad h_{j,\nu,\sigma} = \frac{1}{\sqrt{N_d}} \sum_k e^{+\mathrm{i}kj} h_{k,\nu,\sigma} \,. \tag{4.8}$$

Using the identity

$$\frac{1}{N_d} \sum_j^{N_d} e^{\mathrm{i}j(k'-k)} = \delta_{k,k'} \,, \tag{4.9}$$

we get the diagonal Hamiltonian

$$\begin{aligned} H^{(k)}_{\text{eff}} &= \mathcal{F}\left(H_{\text{eff}}\right) \\ &= E_0 + \sum_{\nu=1}^{2} \sum_\sigma \sum_k \underbrace{\left[a_0 + \sum_{n=1}^{r-2} 2a_n \cos(nk) \right]}_{=:\omega(k)} h^\dagger_{k,\nu,\sigma} h_{k,\nu,\sigma} \,, \end{aligned} \tag{4.10}$$

which defines the single-hole dispersion $\omega(k)$. The dispersions for different orders are almost identical for small λ, because the corrections decrease exponentially in order r with λ^r. We notice, however, a constant difference between the fist-order dispersion $\omega^{(1)}(k)$ and the second-order dispersion $\omega^{(2)}(k)$, which comes from the constant second-order contribution to a_0 in Equation 4.4. This leads to a constant shift of the dispersion by $-\frac{3}{2}\lambda^2$, which can be seen in Figure 4.1, where the dispersion is plotted for $\lambda = 0.1$ in different orders.

4.4. Energy Gap and Critical Parameters

Next, we are interested in the energy gap $\Delta(\lambda)$, which is the energy difference between the ground-state energy from Equation 2.11 and the minimal energy of the one-quasiparticle dispersion, which is located at $k = \pi$. We want to study the quantum critical behaviour and can detect a second-order quantum phase transition by the closing of the gap. For $t = 0$, the gap is finite with $\Delta = \frac{3}{4}$, as this is the energy of one dimer with one hole. For $t \neq 0$, however, it is possible for the gap to close at the critical point λ_c at some coupling ratio $\lambda_c = t/J_\perp$. In order to find the critical point, we calculate the gap via

$$\Delta = \min_k \omega(k) = \omega(k = \pi) \,. \tag{4.11}$$

As can be seen in Figure 4.2, the series of $\Delta(\lambda)$ converges up to a certain point and appears to close somewhere between $\lambda = 0.5$ and $\lambda = 0.6$. Starting at $\lambda = 0.35$, the

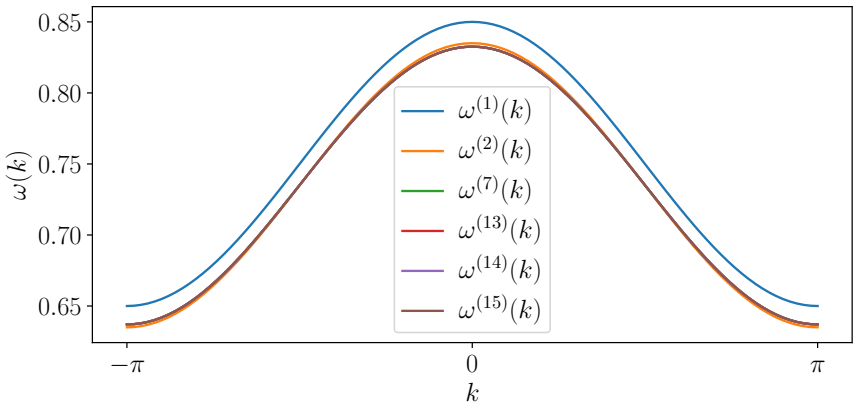

Figure 4.1.: The one-hole dispersion $\omega(k)$ of a mixed dimensional t-$J_\perp$-ladder in different orders for $\lambda = 0.1$. The dispersions have the same periodicity and almost the same amplitude. The shift between order one (blue line) and higher orders stems from a constant local hopping contribution in second order.

bare series diverges and we can not locate λ_c quantitatively. Using Padé and Dlog Padé approximations as described in section 3.2, we can extrapolate it. We calculate the Padé approximants for multiple combinations of L and M and filter out the defective ones. For high enough orders, they converge well and indeed predict a closing of the gap at some λ_c. The three best Padés together with the three highest orders of the gap $\Delta(\lambda)$ are plotted in Figure 4.2.

However, because we can use Padé approximants to accurately determine the critical point only if the gap is closing according to an integer power law, we also need to look at the Dlog Padé approximants, to find the critical exponent $z\nu$. Arranging the Dlog Padés in families as described in section 3.2 and plotting their value for λ_c and $z\nu$ over the order $L + M$ shows, that they converge to the same value, as can be seen in Figure 4.3. An exception poses the family $L - M = 3$, which possibly converges only for orders 14 and upwards. We can, however, not verify it, as our perturbation is only in order 15. We explain the behaviour by the fact, that Padé and Dlog Padé approximants loose accuracy with increasing values for $|L - M|$ as explained in section 3.2. This can also be seen by the relatively high-order convergence of the family $L - M = -3$.

Averaging over the value given by the highest order in each family, we get

$$\lambda_c = 0.52854 \pm 0.00007\,. \tag{4.12}$$

The uncertainty hereby represents the standard deviation of the arithmetic average. When we do the same for the critical exponent, we get

$$z\nu = 1.000 \pm 0.001\,. \tag{4.13}$$

Because we determined that the gap closes indeed with an integer power law ($z\nu = 1$), we can also use the value given by the Padé approximants. As can be seen in Figure 4.4,

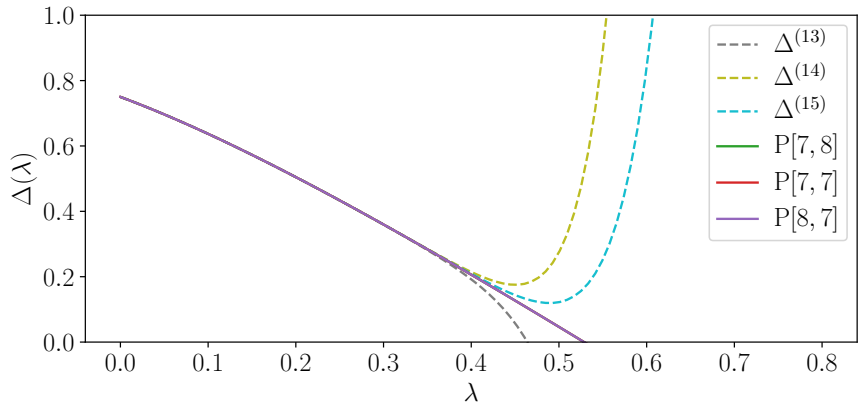

Figure 4.2.: The power series of the gap Δ between the ground-state energy and the minimum of the one-hole dispersion in orders 13, 14 and 15 as dashed lines. The series is extrapolated by the Padé approximants P $[7, 8]$, P $[7, 7]$ and P $[8, 7]$ (solid lines). The bare series diverges but the approximants converge almost identically. They predict a closing of the gap and can be used to locate the critical point λ_c where $\Delta(\lambda_c) = 0$.

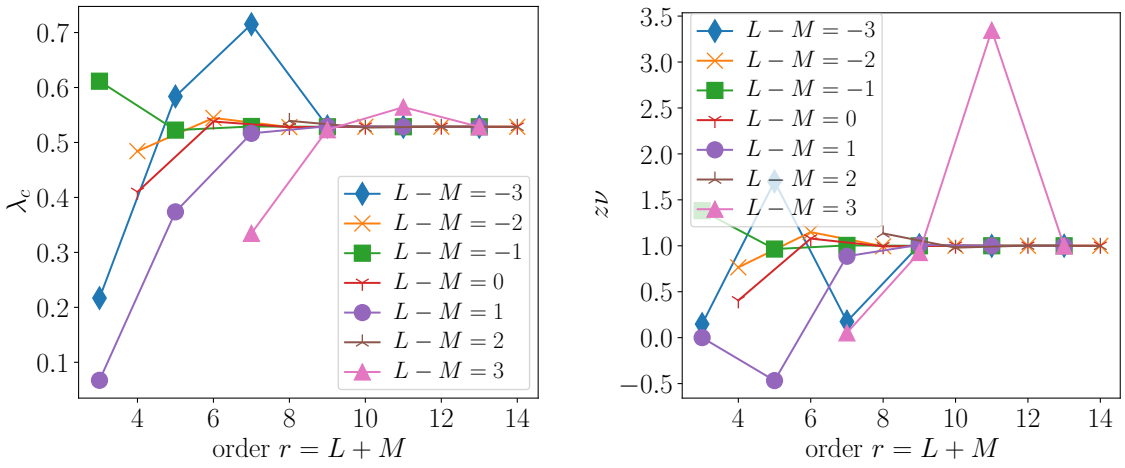

Figure 4.3.: The quantum critical point λ_c (left) and the critical exponent $z\nu$ (right) calculated using different Dlog Padé approximants. The approximants are grouped into families with $L - M =$ const. and the results are plotted over the order $r = L + M$. With increasing order, the families converge to the same values for λ_c and $z\nu$. As expected, the families with the highest absolute value for $L - M$ (blue and pink) converge only at higher orders than the other families. The quantitative values for λ_c and $z\nu$ are obtained by taking the arithmetic average over the highest-order values for each family.

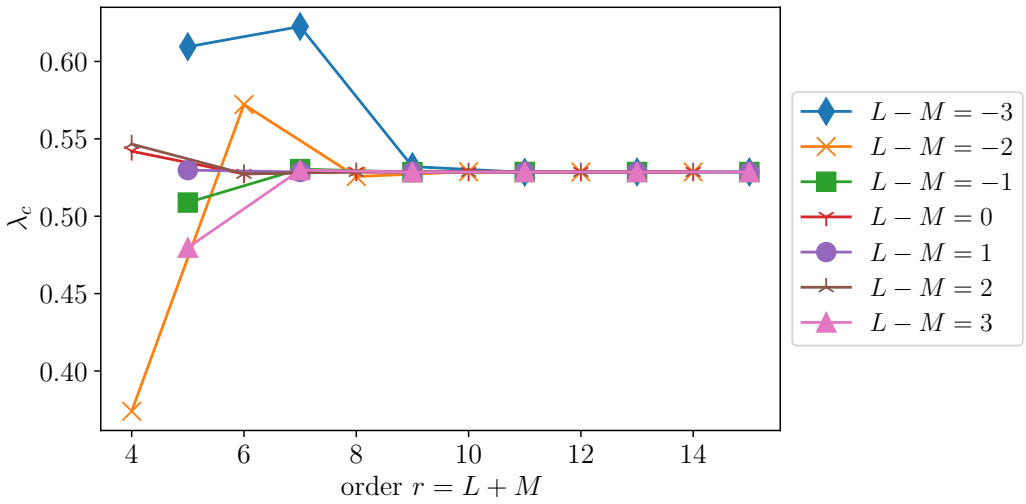

Figure 4.4.: The quantum critical point λ_c calculated using different Padé approximants. In analogy with Figure 4.3, the approximants are grouped into families with $L - M = \text{const.}$ and the results are plotted over the order $r = L + M$. With increasing order, the families converge to the same value for λ_c. The quantitative value for λ_c is obtained by taking the arithmetic average over the highest-order values for each family. Because every family converges at lower orders when compared to the Dlog Padé approximants, the standard deviation of the average is smaller, reducing the uncertainty.

the different families also converge well with increasing orders. Averaging over the value given by the highest order in each family yields

$$\lambda_c = 0.5285693 \pm 0.0000007\,. \tag{4.14}$$

This is the same value as we get from our Dlog Padés, however, with a considerably smaller uncertainty. This is because the families start to converge for much lower orders already for our Padés, when compared to the Dlog Padés.

Knowing the critical exponent $z\nu = 1$ enables us to make statements about the universality class of the quantum phase transition. To our knowledge, there are two universality classes, where the product of the dynamical exponent z and the correlation length exponent ν is equal to one. The first is the universality class of the $2D$ transverse field Ising model, where $z = \nu = 1$ [24, 25, 26]. The second is the universality class of the two-dimensional XY model, where $z = 1$ and $\nu = \frac{1}{2}$ [27, 26]. Determining the exact universality class, however, is not possible with our results. In the next chapter we discuss ways to find it in the future.

5. Conclusions and Outlook

In this Bachelor's thesis, we studied a mixed-dimensional t-$J_\perp$-ladder doped with one hole from the limit of isolated rungs. We transformed the initial non-diagonal Hamiltonian H, which contains nearest-neighbour hopping terms of the hole, into an effective Hamiltonian H_{eff} using the method of perturbative continuous unitary transformations (pCUTs). This effective Hamiltonian is block diagonal, as it conserves the number of triplet excitations, which allows us to study the behaviour of holes in the absence of triplet excitations.

From the one-hole block of the effective Hamiltonian, we determined the one-hole hopping amplitudes, allowing us to rewrite it into a normal-ordered form using operators that only describe the hopping of the hole and the spin in the same rung. We diagonalized the one-hole block of H_{eff} by going into momentum space using Fourier transformation and obtained the one-hole dispersion $\omega(k)$. From the dispersion, we calculated a series in order 15 in the perturbation parameter $\lambda = t/J_\perp$ of the gap Δ between the ground-state energy and the minimal energy of the one-hole dispersion, which is located at momentum $k = \pi$. We extrapolated the perturbative series using Padé and Dlog Padé approximants and found that it closes at the quantum phase transition point $\lambda_c = 0.5285693 \pm 0.0000007$. In the last step, we used our Dlog Padé approximants to determine the critical exponent according to which the gap closes to be $z\nu = 1.000 \pm 0.001$. This allowed us to limit possible scenarios of a quantum phase transition to either two-dimensional Ising or $2D$-XY universality.

Fully determining the universality class would be possible by finding an exact value for either z or ν and not just their product. One way to achieve this would be to calculate z by evaluating the dispersion $\omega(k, \lambda)$ at $\lambda = \lambda_c$ and studying the k-dependence around the minimum at $k = \pi$ [24]. Another way would be to calculate an observable of the system, and/or use a different approach than pCUTs.

In order to be able to make predictions about a possible superconducting phase in the system, we would need to increase the doping to two (or more) holes. This would allow us to make predictions about possible bound states and attractive couplings between holes, which could be used to explain the results of the experiment conducted in Ref. [13]. To make predictions about how the system describes the new superconductor $La_3Ni_2O_7$, we would need to extend the ladder system into a two-dimensional bilayer, as this is the geometry conjectured to be present in the material [7]. Because real systems are never perfect and magnetic coupling and hole hopping never take place completely in separate directions, it is also worth studying the stability of our results against the presence of finite $t_\perp$ and $J_\parallel$.

A. Hopping Amplitudes

n	a_n
0	$1014.43685294176\lambda^{14} + 137.844119715051\lambda^{12} - 49.8621695059316\lambda^{10}$ $-1.25048828125001\lambda^8 + 2.8828125\lambda^6 - 0.28125\lambda^4 - 0.75\lambda^2 + 3/4$
1	$-373.169587481308\lambda^{15} + 1128.69839056822\lambda^{13} - 85.1606470949461\lambda^{11}$ $-35.9323120117188\lambda^9 + 7.68896484375\lambda^7 + 1.265625\lambda^5 - 1.125\lambda^3 + 0.5\lambda$
2	$1862.71461785981\lambda^{14} + 141.265625610963\lambda^{12} - 77.1461587599765\lambda^{10}$ $+2.8544921875\lambda^8 + 3.134765625\lambda^6 - 0.75\lambda^4$
3	$1056.15438400532\lambda^{15} + 608.776564352009\lambda^{13} - 92.2040113558984\lambda^{11}$ $-8.843578197337 96\lambda^9 + 4.31396484375\lambda^7 - 0.46875\lambda^5$
4	$1149.34714293217\lambda^{14} - 48.7818835049008\lambda^{12} - 24.2023684654707\lambda^{10}$ $+4.66845703125\lambda^8 - 0.28125\lambda^6$
5	$1423.16455868445\lambda^{15} + 66.2197708114916\lambda^{13} - 39.0690702352014\lambda^{11}$ $+4.390869140625\lambda^9 - 0.1640625\lambda^7$
6	$241.418539244369\lambda^{14} - 50.2366425575707\lambda^{12} + 3.75817108154297\lambda^{10}$ $-0.09375\lambda^8$
7	$447.386752153611\lambda^{15} - 56.2017802715738\lambda^{13} + 3.00358772277832\lambda^{11}$ $-0.052734375\lambda^9$
8	$-57.015713040412\lambda^{14} + 2.2780179977417\lambda^{12} - 0.029296875\lambda^{10}$
9	$-53.7163884598689\lambda^{15} + 1.65752291679382\lambda^{13} - 0.01611328125\lambda^{11}$
10	$1.16603019833565\lambda^{14} - 0.0087890625\lambda^{12}$
11	$0.797611467540264\lambda^{15} - 0.0047607421875\lambda^{13}$
12	$-0.0025634765625\lambda^{14}$
13	$-0.001373291015625\lambda^{15}$
14	0
15	0

Table A.1.: Transition amplitudes a_n for hopping by $n = 1, ..., 15$ sites of the effective one-hole Hamiltonian in order $r = 15$.

Bibliography

[1] H. Kamerlingh Onnes. "Further experiments with liquid helium. C. On the change of electric resistance of pure metals at very low temperatures etc. IV. The resistance of pure mercury at helium temperatures". In: *Koninklijke Nederlandse Akademie van Wetenschappen Proceedings Series B Physical Sciences* 13 (Jan. 1911), pp. 1274–1276.

[2] J. G. Bednorz and K. A. Müller. "Possible highTc superconductivity in the Ba-La-Cu-O system". In: *Zeitschrift für Physik B Condensed Matter* 64.2 (1986), pp. 189–193. DOI: 10.1007/BF01303701. URL: https://doi.org/10.1007/BF01303701.

[3] J. Bardeen. "Theory of the Meissner Effect in Superconductors". In: *Phys. Rev.* 97 (6 Mar. 1955), pp. 1724–1725. DOI: 10.1103/PhysRev.97.1724. URL: https://link.aps.org/doi/10.1103/PhysRev.97.1724.

[4] J. Bardeen, L. N. Cooper, and J. R. Schrieffer. "Theory of Superconductivity". In: *Phys. Rev.* 108 (5 Dec. 1957), pp. 1175–1204. DOI: 10.1103/PhysRev.108.1175. URL: https://link.aps.org/doi/10.1103/PhysRev.108.1175.

[5] Jozef Spalek. *t-J model then and now: A personal perspective from the pioneering times*. 2007. arXiv: 0706.4236 [cond-mat.str-el].

[6] Fabian Grusdt et al. "Meson formation in mixed-dimensional t-J models". In: *SciPost Physics* 5.6 (Dec. 2018). DOI: 10.21468/scipostphys.5.6.057. URL: http://dx.doi.org/10.21468/SciPostPhys.5.6.057.

[7] Chen Lu et al. *Interlayer Coupling Driven High-Temperature Superconductivity in $La_3Ni_2O_7$ Under Pressure*. 2023. arXiv: 2307.14965 [cond-mat.supr-con].

[8] T. M. Rice. "t-J ladders and cuprate ladder compounds". In: *Zeitschrift für Physik B Condensed Matter* 103.2 (1996), pp. 165–172. DOI: 10.1007/s002570050353. URL: https://doi.org/10.1007/s002570050353.

[9] E. Dagotto, J. Riera, and D. Scalapino. "Superconductivity in ladders and coupled planes". In: *Phys. Rev. B* 45 (10 Mar. 1992), pp. 5744–5747. DOI: 10.1103/PhysRevB.45.5744. URL: https://link.aps.org/doi/10.1103/PhysRevB.45.5744.

[10] Zheng Zhu et al. "Nature of strong hole pairing in doped Mott antiferromagnets". In: *Scientific Reports* 4.1 (June 2014). ISSN: 2045-2322. DOI: 10.1038/srep05419. URL: http://dx.doi.org/10.1038/srep05419.

[11] Hannah Lange et al. "Feshbach resonance in a strongly repulsive ladder of mixed dimensionality: A possible scenario for bilayer nickelate superconductors". In: *Phys. Rev. B* 109 (4 Jan. 2024), p. 045127. DOI: 10.1103/PhysRevB.109.045127. URL: https://link.aps.org/doi/10.1103/PhysRevB.109.045127.

[12] Hannah Lange et al. *Pairing dome from an emergent Feshbach resonance in a strongly repulsive bilayer model*. 2023. arXiv: 2309.13040 [cond-mat.str-el].

[13] Sarah Hirthe et al. "Magnetically mediated hole pairing in fermionic ladders of ultracold atoms". In: *Nature* 613.7944 (2023), pp. 463–467. DOI: 10.1038/s41586-022-05437-y. URL: https://doi.org/10.1038/s41586-022-05437-y.

[14] Kai Phillip Schmidt. "Spectral Properties of Quasi One-dimensional Quantum Antiferromagnets . Perturbative Continuous Unitary Transformations". PhD thesis. Universität zu Köln, 2004. URL: https://kups.ub.uni-koeln.de/1316/.

[15] Sebastian Duffe. "Effective hamiltonians for undoped and hole-doped antiferromagnetic spin-$\frac{1}{2}$ ladders by self-similar continuous unitary transformations in real space". In: (Aug. 2010). DOI: 10.17877/DE290R-14712.

[16] M Takahashi. "Half-filled Hubbard model at low temperature". In: *Journal of Physics C: Solid State Physics* 10.8 (Apr. 1977), p. 1289. DOI: 10.1088/0022-3719/10/8/031. URL: https://dx.doi.org/10.1088/0022-3719/10/8/031.

[17] Per-Olov Löwdin. "Studies in Perturbation Theory. IV. Solution of Eigenvalue Problem by Projection Operator Formalism". In: *Journal of Mathematical Physics* 3.5 (Dec. 2004), pp. 969–982. ISSN: 0022-2488. DOI: 10.1063/1.1724312. eprint: https://pubs.aip.org/aip/jmp/article-pdf/3/5/969/11115142/969_1_online.pdf. URL: https://doi.org/10.1063/1.1724312.

[18] J. R. Schrieffer and P. A. Wolff. "Relation between the Anderson and Kondo Hamiltonians". In: *Phys. Rev.* 149 (2 Sept. 1966), pp. 491–492. DOI: 10.1103/PhysRev.149.491. URL: https://link.aps.org/doi/10.1103/PhysRev.149.491.

[19] C. Knetter and G.S. Uhrig. "Perturbation theory by flow equations: dimerized and frustrated S = 1/2 chain". In: *The European Physical Journal B - Condensed Matter and Complex Systems* 13.2 (Jan. 2000), pp. 209–225. ISSN: 1434-6036. DOI: 10.1007/s100510050026. URL: http://dx.doi.org/10.1007/s100510050026.

[20] D. Klagges. "Effektive Zweispinmodelle für Cluster-State-Hamilton-Operatoren". Diploma Thesis. TU Dortmund, 2011.

[21] Subir Sachdev. *Quantum Phase Transitions*. 2nd ed. Cambridge University Press, 2011.

[22] A. J. Guttmann. "Asymptotic Analysis of Power-Series Expansions". In: *Phase Transitions and Critical Phenomena*. Ed. by C. Domb, M. S. Green, and J. L. Lebowitz. Vol. 13. Academic Press, 1989.

[23] George A. Baker. "Chapter 1 The Padé Approximant Method and Some Related Generalizations**Work performed in part under the auspices of the U.S. Atomic Energy Commission." In: *The Padé Approximant in Theoretical Physics*. Ed. by GEORGE A. BAKER and JOHN L. GAMMEL. Vol. 71. Mathematics in Science and Engineering. Elsevier, 1970, pp. 1–39. DOI: https://doi.org/10.1016/S0076-5392(08)62672-7. URL: https://www.sciencedirect.com/science/article/pii/S0076539208626727.

[24] Patrick Adelhardt. "Quantum criticality of long-range generalized quantum spin systems". MA thesis. Institute for Theoretical Physics I, Friedrich-Alexander-Universität Erlangen-Nürnberg, May 2020.

[25] Géza Ódor. "Universality classes in nonequilibrium lattice systems". In: *Rev. Mod. Phys.* 76 (3 Aug. 2004), pp. 663–724. DOI: 10.1103/RevModPhys.76.663. URL: https://link.aps.org/doi/10.1103/RevModPhys.76.663.

[26] Kedar Damle and Subir Sachdev. "Multicritical Crossovers near the Dilute Bose Gas Quantum Critical Point". In: *Phys. Rev. Lett.* 76 (23 June 1996), pp. 4412–4415. DOI: 10.1103/PhysRevLett.76.4412. URL: https://link.aps.org/doi/10.1103/PhysRevLett.76.4412.

[27] P. Ray and B.K. Chakrabarti. "Exact ground-state excitations of the XY model in a transverse field in one dimension". In: *Physics Letters A* 98.8 (1983), pp. 431–432. ISSN: 0375-9601. DOI: https://doi.org/10.1016/0375-9601(83)90255-4. URL: https://www.sciencedirect.com/science/article/pii/0375960183902554.

Danksagung

An dieser Stelle möchte ich meinen Dank all denen aussprechen, die es mir ermöglicht haben diese Arbeit durchzuführen. Besonderer Dank gilt Professor Kai Phillip Schmidt für die exzellente Betreuung und die Möglichkeit, bei ihm eine Bachelorarbeit zu verfassen. Des Weiteren möchte ich mich bei Patrick Adelhardt und Paul Fadler bedanken, die mir bei Fragen stets zur Verfügung standen. Ebenso möchte ich mich bei der gesamten Arbeitsgruppe für das herausragende Arbeitsklima und die tolle gemeinsame Zeit bedanken. Schlussendlich gilt mein Dank all denen, die die Arbeit korrekturgelesen haben, und natürlich meinen Eltern, die mir das Studium ermöglichen und mich stets unterstützen.

Eidesstattliche Versicherung

Hiermit versichere ich, dass ich die vorliegende Arbeit selbstständig verfasst und keine anderen als die angegebenen Quellen und Hilfsmittel benutzt habe, dass alle Stellen der Arbeit, die wörtlich oder sinngemäß aus anderen Quellen übernommen wurden, als solche kenntlich gemacht sind und dass die Arbeit in gleicher oder ähnlicher Form noch keiner Prüfungsbehörde vorgelegt wurde.

Erlangen, den 9. Februar 2024 Jakob Heidweiler